Inorg. Chem. **2005**, *44*, 8459–8468

Homoleptic Trimethylsilylacetylide Complexes of Chromium(III), Iron(II), and Cobalt(III): Syntheses, Structures, and Ligand Field Parameters

Louise A. Berben and Jeffrey R. Long*

Contribution from the Department of Chemistry, University of California, Berkeley California 94720-1460

Received September 10, 2005

A straightforward method for synthesizing soluble homoleptic trimethylsilylacetylide complexes of first-row transition metal ions is presented. Reaction of anhydrous $CrCl_2$ with an excess of $LiCCSiMe_3$ in THF at −25 °C affords orange $Li_3[Cr(CCSiMe_3)_6]\cdot 6THF$ (**1**), while analogous reactions employing $M(CF_3SO_3)_2$ (M = Fe or Co) generate pale yellow $Li_4[Fe(CCSiMe_3)_6]\cdot 4LiCCSiMe_3\cdot 4Et_2O$ (**2**) and colorless $Li_3[Co(CCSiMe_3)_6]\cdot 6THF$ (**3**). Slightly modified reaction conditions lead to $Li_8[Cr_2O_4(CCSiMe_3)_6]\cdot 6LiCCSiMe_3\cdot 4glyme$ (**4**), featuring a bis-μ-oxo-bridged binuclear complex, and $Li_3[Co(CCSiMe_3)_5(CCH)]\cdot LiCF_3SO_3\cdot 8THF$ (**5**). The crystal structures of **1**–**3** show the trimethylsilylacetylide complexes to display an octahedral coordination geometry, with M–C distances of 2.077(3), 1.917(7)–1.935(7), and 1.908(3) Å for M = Cr^{III}, Fe^{II}, and Co^{III}, respectively, and nearly linear M–C≡C angles. The UV–visible absorption spectrum of $[Cr(CCSiMe_3)_6]^{3-}$ in hexanes exhibits one spin-allowed d–d transition ($^4T_{2g} \leftarrow {}^4A_{1g}$) and three lower-energy spin-forbidden d–d transitions. The spectra of $[Fe(CCSiMe_3)_6]^{4-}$ and $[Co(CCSiMe_3)_6]^{3-}$ in acetonitrile display high-intensity charge-transfer bands, which obscure all d–d transitions except for the lowest-energy spin-allowed band ($^1T_{1g} \leftarrow {}^1A_{1g}$) of the latter complex. Time-dependent density functional theory (TD-DFT) calculations were employed as an aide in assigning the observed transitions. Taken together, the results are most consistent with the ligand field parameters Δ_o = 20 200 cm^{-1} and B = 530 cm^{-1} for $[Cr(CCSiMe_3)_6]^{3-}$, Δ_o = 32 450 cm^{-1} and B = 460 cm^{-1} for $[Fe(CCSiMe_3)_6]$,$^{4-}$ and Δ_o = 32 500 cm^{-1} and B = 516 cm^{-1} for $[Co(CCSiMe_3)_6]^{3-}$. Ground-state DFT calculations support the conclusion that trimethylsilylacetylide acts as a π-donor ligand.

Introduction

Pure carbon bridges such as acetylenediide, $C{\equiv}C^{2-}$, and 1,3-butadiynediide, $C{\equiv}C{-}C{\equiv}C^{2-}$, are of significant current interest as linear connectors facilitating electronic communication between metal centers.[1] Our motivation for studying these bridging ligands derives in particular from their potential as cyanide replacement units capable of mediating strong magnetic exchange coupling. While the magnitude of the exchange coupling through such species has never been measured, their symmetric nature and more negative charge compared with cyanide lead us to expect an increase in orbital overlap between bridge and metal, and hence, enhanced magnetic exchange coupling. Indeed, molecules such as $[I(dmpe)_2Mn{-}C{\equiv}C{-}C{\equiv}C{-}Mn(dmpe)_2I]^{2-}$ and $[Cp^*(dppe)Fe{-}C{\equiv}C{-}C{\equiv}C{-}Fe(dppe)Cp^*]^{2-}$,[2] which are diamagnetic at 295 K despite their paramagnetic end groups, provide direct confirmation of the notion that coupling through a pure carbon bridge can be exceptionally strong.

Hexacyano complexes of first-row transition metal ions have served extensively as precursors to both high-spin, cyano-bridged molecules[3] and magnetic Prussian blue-type solids.[4] Although certain analogous acetylide complexes $[M(C{\equiv}CR)_6]^{n-}$ (R = H, Me, or Ph) have long been known,[5] they are reported as highly unstable and/or insoluble salts, ill-suited for use in subsequent bridge-forming reactions.

* To whom correspondence should be addressed. E-mail: jrlong@berkeley.edu.

(1) (a) Paul, F.; Lapinte, C. *Coord. Chem. Rev.* **1998**, *178*−*180*, 431. (b) Bruce, M. I.; Low, P. J.; Costuas, K.; Halet, J.-F.; Best, S. P.; Heath, G. A. *J. Am. Chem. Soc.* **2000**, *122*, 1949. (c) Dembinski, R.; Bartik, T.; Bartik, B.; Jaeger, M.; Gladysz, J. A. *J. Am. Chem. Soc.* **2000**, *122*, 810. (d) Fernández, F. J.; Venkatesan, K.; Blacque, O.; Alfonso, M.; Schmalle, H. W.; Berke, H. *Chem. Eur. J.* **2003**, *9*, 6192.

(2) (a) Fernandez, F. J.; Blaque, O.; Alfonso, M.; Berke, H. *Chem. Commun.* **2001**, 1266. (b) Le Narvour, N.; Toupet, L.; Lapinte, C. *J. Am. Chem. Soc.* **1995**, *117*, 7129.

10.1021/ic051551z CCC: $30.25
Published on Web 10/21/2005

Complexes of this type are known for M = Cr^{III},[6] Mn^{III},[7] Fe^{II},[8] Fe^{III},[8] Co^{II},[9] and Co^{III},[10] with the only difference in stoichiometry, color, and magnetism from the hexacyano species corresponding to the existence of high-spin $[Co(CCR)_6]$,[4−9] as opposed to low-spin $[Co(CN)_4]^{2-}$ and $[Co(CN)_5]^{3-}$.[11,12] A similar parallel to cyanide chemistry occurs for the late transition metals, for which the complexes $[M(CCR)_4]^{2-}$ (M = Ni, Pd, Pt) are diamagnetic and presumably square planar,[13] the complexes $[M(CCR)_2]^-$ (M = Cu, Ag, Au) are presumably linear,[14] and the complexes $[M(CCR)_4]^{2-}$ (M = Zn, Cd, Hg) are tetrahedral.[15,16] Due to their highly reactive nature, the only characterization data available for most of these homoleptic acetylide complexes are magnetic moments and infrared spectra. Exceptions to this are the structurally characterized tetrahedral species $[M(CCH)_4]^{2-}$ (M = Zn, Cd).[16] In addition, the use of a bulky substituent R permitted isolation and crystallographic characterization of octahedral $[M(CCSi^tBu_3)_6]^{2-}$ (M = Zr, Hf) and trigonal prismatic $[Ta(CCSi^tBu_3)_6]^-$.[17]

Further impetus for developing a synthetic route to soluble first-row transition metal−acetylide complexes is provided by a desire to probe further the nature of metal−alkynyl bonding. Historically, the electronic properties of the acetylide ligand were interpreted by comparisons with the isoelectronic cyanide ligand. It was generally accepted to be similar in character, albeit with a weaker π-acceptor contribution. More recently, however, a variety of investigations have led to contradictory conclusions.[18] Photoelectron spectroscopy studies on late transition metal−acetylide complexes with cyclopentadienyl-based capping ligands, for example $[Cp(CO)_2Fe(CCH)]$, led to the conclusion that the acetylide ligand was a strong σ donor, weak π donor, and similar in character to a chloride ligand.[19] Density functional theory (DFT) studies on first-row acetylide-bridged dimers concluded that the bonding of early transition metal complexes with ancillary π-donor ligands, where there was evidence for π-acceptor and π-donor character, was very different to the bonding predicted for late metal complexes with ancillary π-acceptor ligands, where there was no evidence for π-acceptor or π-donor character.[20] Additional attempts at characterizing the bonding have employed X-ray structural comparisons,[18] electronic absorption,[21] and infrared[18] and NMR spectroscopy.[22] While these studies provide some insight, it has been suggested that the nature (i.e., π-acceptor vs π-donor) of the ancillary ligands in these complexes has a pronounced effect on the nature and strength of the metal−alkynyl interaction, and ultimately a general description of the nature of metal−alkynyl bonding has not been developed.[18] Given the importance of the metal−cyanide π interaction in promoting magnetic exchange coupling,[23] we wished to establish whether the metal−alkynyl π interaction in first-row transition metal complexes would be of a suitable nature and strength to facilitate our aims.

Herein, we report a straightforward method for synthesizing the soluble, homoleptic species $[Cr(CCSiMe_3)_6]^{3-}$, $[Fe(CCSiMe_3)_6]$,[4−] and $[Co(CCSiMe_3)_6]^{3-}$, together with their structural and spectroscopic properties.

Experimental Section

Preparation of Compounds. All manipulations were performed under a nitrogen atmosphere using standard Schlenk line and glovebox techniques. Syntheses of $Fe(CF_3SO_3)_2 \cdot MeCN$[24] and $Co(CF_3SO_3)_2$[25] were carried out as reported previously. Diethyl ether and acetonitrile were passed over alumina and degassed prior to use. Tetrahydrofuran, benzene, hexanes, and glyme were purchased in Sure/Seal bottles, stored over 3 Å molecular sieves, and degassed prior to use. Trimethylsilylethyne was degassed by three freeze−pump−thaw cycles and stored over 3 Å molecular sieves. All other reagents were used without further purification.

$Li_3[Cr(CCSiMe_3)_6] \cdot 6THF$ (1). A solution of $LiCCSiMe_3$ was generated by adding ^{n}BuLi (23 mL, 59 mmol, 2.5 M hexane solution) to a solution of $HCCSiMe_3$ (9.2 mL, 65 mmol) in 50 mL of THF at −25 °C. After being stirred at room temperature for 1

(3) (a) Mallah, T.; Auberger, C.; Verdaguer, M.; Veillet, P. *J. Chem. Soc., Chem. Commun.* **1995**, 61. (b) Van Langenberg, K.; Batten, S. R.; Berry, K. J.; Hockless, D. C. R.; Moubaraki, B.; Murray, K. S. *Inorg. Chem.* **1997**, *36*, 5006. (c) Marvaud, V. C.; Decroix, A.; Scuiller, A.; Guyard-Duhayon, C. J.; Vaissermann, C.; Gonnet, F.; Verdaguer, M. *Chem. Eur. J.* **2003**, *9*, 1678. (d) Berlinguette, C. P.; Vaughn, D.; Cañada-Vilalta, C.; Galán-Mascarós, J. R.; Dunbar, K. R. *Angew. Chem., Int. Ed.* **2003**, *42*, 1523. (e) Choi, H. J.; Sokol, J. J.; Long, J. R. *Inorg. Chem.* **2004**, *43*, 1606.

(4) (a) Mallah, T.; Thiébaut, S.; Verdaguer, M.; Veillet, P. *Science* **1993**, *262*, 1554. (b) Entley, W. R.; Girolami, G. S. *Science* **1995**, *268*, 397. (c) Ferlay, S.; Mallah, T.; Ouahès, R.; Veillet, P.; Verdaguer, M. *Nature* **1995**, *378*, 701. (d) Holmes, S. M.; Girolami, G. S. *J. Am. Chem. Soc.* **1999**, *121*, 5593.

(5) Nast, R. *Coord. Chem. Rev.* **1982**, *47*, 89 and references therein.

(6) Nast, R.; Sirtl, E. *Chem. Ber.* **1955**, *88*, 1723.

(7) Nast, R.; Griesshammer, H. *Chem. Ber.* **1957**, *90*, 1315.

(8) Nast, R.; Urban, F. *Z. Anorg. Allg. Chem.* **1956**, *287*, 17.

(9) Nast, R.; Fock, K. *Chem. Ber.* **1976**, *109*, 455.

(10) Nast, R.; Lewinsky, H. *Z. Anorg. Allg. Chem.* **1955**, *282*, 210.

(11) (a) Carter, S. J.; Foxman, B. M.; Stuhl, L. S. *J. Am. Chem. Soc.* **1984**, *106*, 4265. (b) Alexander, J. J.; Gray, H. B. *J. Am. Chem. Soc.* **1967**, *89*, 3356. (c) Brown, L. D.; Raymond, K. N. *Inorg. Chem.* **1975**, *14*, 2590.

(12) Additionally, a hexaacetylide complex of Cr^{II} analogous to low-spin $[Cr(CN)_6]^{4-}$ is not known: (a) Ljungstrom, E. *Acta Chem. Scand.* **1977**, *A31*, 104. (b) Eaton, J. P.; Nicholls, D. *Transition Met. Chem.* **1981**, *6*, 203.

(13) (a) Taube, R.; Honymus, G. *Angew. Chem.* **1975**, *87*, 291. (b) Barral, C.; Jimenez, R.; Royer, E.; Moreno, V.; Santos, A. *Inorg. Chim. Acta* **1978**, *31*, 165.

(14) (a) Nast, R.; Pfab, W. *Chem. Ber.* **1956**, *89*, 415. (b) Nast, R.; Schindel, H. *Z. Anorg. Allg. Chem.* **1963**, *326*, 201. (c) Nast, R.; Kirner, U. *Z. Anorg. Allg. Chem.* **1964**, *330*, 311.

(15) (a) Nast, R.; Muller, R. *Chem. Ber.* **1958**, *91*, 2861. (b) Nast, R.; Richers, C. *Z. Anorg. Allg. Chem.* **1963**, *319*, 320. (c) Nast, R.; Richers, C. *Chem. Ber.* **1964**, *97*, 3317.

(16) (a) Weiss, E.; Plass, H. *J. Organomet. Chem.* **1968**, *14*, 21. (b) Cremer, U.; Pantenburg, I.; Ruschewitz. U. *Inorg. Chem.* **2003**, *42*, 7716.

(17) Vaid, T. P.; Veige, A. S.; Lobkovsky, E. B.; Glassey, W. V.; Wolczanski, P. T.; Liable-Sands, L. M.; Rheingold, A. L.; Cundari, T. R. *J. Am. Chem. Soc.* **1998**, *120*, 10067.

(18) Manna, J.; John, K. D.; Hopkins, M. D. *Adv. Organomet. Chem.* **1995**, *38*, 79 and references therein.

(19) (a) Lichtenberger, D. L.; Renshaw, S. K.; Bullock, R. M. *J. Am. Chem. Soc.* **1993**, *115*, 3276. (b) Lichtenberger, D. L.; Renshaw, S. K. *Organometallics* **1993**, *12*, 3522.

(20) Belanzoni, P.; Re, N.; Sgamellotti, A.; Floriani, C. *Dalton Trans.* **1997**, 4773.

(21) (a) Stoner, T. C.; Geib, S. J.; Hopkins, M. D. *Angew. Chem., Int. Ed. Engl.* **1993**, *32*, 409. (b) Stoner, T. C.; Geib, S. J.; Hopkins, M. D. *J. Am. Chem. Soc.* **1992**, *114*, 4201. (c) Stoner, T. C.; Dallinger R. F.; Hopkins, M. D. *J. Am. Chem. Soc.* **1990**, *112*, 5651.

(22) Wrackmeyer, B.; Horchler, K. *Prog. NMR Spectrosc.* **1990**, *22*, 209.

(23) Weihe, H.; Güdel, H. U. *Comments Inorg. Chem.* **2000**, *22*, 356.

(24) Blakesley, D. W.; Payne, S. C.; Hagen, K. S. *Inorg. Chem.* **2000**, *39*, 1979.

(25) Byington, A. R.; Bull, W. E. *Inorg. Chim. Acta*. **1977**, *21*, 239.

Table 1. Crystallographic Data[a] for the Homoleptic Complexes $Li_3[Cr(CCSiMe_3)_6]\cdot 6THF$ (**1**), $Li_4[Fe(CCSiMe_3)_6]\cdot 4LiCCSiMe_3\cdot 4Et_2O$ (**2**), $Li_3[Co(CCSiMe_3)_6]\cdot 6THF$ (**3**), $Li_8[Cr_2O_4(CCSiMe_3)_6]\cdot 6LiCCSiMe_3\cdot 4Glyme$ (**4**), and $Li_3[Co(CCSiMe_3)_5(CCH)]\cdot LiCF_3SO_3\cdot 8THF$ (**5**)

	1	**2**	**3**	**4**	**5**
formula	$C_{54}H_{102}CrLi_3O_6Si_6$	$C_{66}H_{130}FeLi_8O_4Si_{10}$	$C_{54}H_{102}CoLi_3O_6Si_6$	$C_{76}H_{148}Cr_2Li_{14}O_{12}Si_{12}$	$C_{60}H_{110}CoLi_4O_{11}SSi_5$
fw	1088.72	1379.97	1095.65	1792.18	1323.68
T, K	135	124	115	113	120
space group	$Pa\bar{3}$	$P2_1/c$	$Pa\bar{3}$	Pn	$P2_1$
Z	6	4	6	2	2
a, Å	19.0415(3)	21.577(14)	18.8534(13)	14.258(5)	13.2891(14)
b, Å		20.956(14)		17.936(6)	23.551(2)
c, Å		20.697(10)		22.374(8)	13.6985(14)
β, deg		103.26(8)		95.467(12)	117.047(2)
V, Å^3	6904.0(2)	9070(9)	6701.5980	5696(4)	3811.8(7)
d_{calc}, g/cm^3	1.259	1.011	1.316	1.045	1.153
R1 (wR2),[b] %	3.74 (10.46)	6.50 (14.07)	4.78 (11.65)	5.08 (13.44)	5.37 (11.56)

[a] Obtained with graphite-monochromated Mo Kα (λ = 0.71073 Å) radiation. [b] $R1 = \Sigma||F_o|-F_c||/\Sigma|F_o|$, $wR2 = \{\Sigma[w(F_o^2-F_c^2)^2]/\Sigma[w(F_o^2)^2]\}^{1/2}$.

h, the solution was cooled back to −25 °C and anhydrous $CrCl_2$ (0.80 g, 6.5 mmol) was added. Upon warming to room temperature and being stirred for 10 h, a dark orange solution formed. Storage of the solution at −25 °C for 3 days afforded a dark orange precipitate, which was collected by filtration and dried under dinitrogen. Additional solid was obtained by concentrating the filtrate to a volume of 20 mL and rechilling. Cooling a saturated THF solution of the combined solids to −25 °C for 1 week gave 2.9 g (44%) of product as orange, octahedron-shaped crystals suitable for X-ray analysis. Absorption spectrum (hexanes): λ_{max} (ϵ_M) 228 (sh, 12 700), 304 (9260), 403 (7440), 494 (1110), 617 (18), 725 (12), 750 (16) nm. Absorption spectrum (MeCN): λ_{max} (ϵ_M) 236 (64 500), 244 (72 500), 253 (134 000), 306 (8810), 317 (8970), 337 (sh, 5670) nm. IR (solid, ATR): ν_{CC} 1998 (m), ν_{CSi} 839 (s) cm^{-1}. μ_{eff} = 3.85 μ_B at 295 K. ES$^-$-MS (MeCN): *m*/*z* 648 ([**1** − Li − 6THF]$^-$). Anal. Calcd for $C_{54}H_{102}CrLi_3O_6Si_6$: C, 59.57; H, 9.44. Found: C, 57.41; H, 9.30. This compound is soluble in polar and nonpolar solvents but decomposes in protic solvents such as methanol.

$Li_4[Fe(CCSiMe_3)_6]\cdot 4LiCCSiMe_3\cdot 4Et_2O$ (2). A solution of $LiCCSiMe_3$ was generated by adding ^{n}BuLi (19 mL, 48 mmol, 2.5 M hexane solution) to a solution of $HCCSiMe_3$ (6.8 mL, 48 mmol) in 50 mL of diethyl ether at −25 °C. After being stirred at room temperature for 1 h, the solution was cooled back to −25 °C, $Fe(CF_3SO_3)_2\cdot$MeCN (2.0 g, 4.8 mmol) was added, and the mixture was then stirred for 20 h at room temperature. Subsequent storage at −25 °C for 24 h resulted in an off-white precipitate, which was collected by filtration and washed with 10 mL of diethyl ether. Addition of 400 mL of benzene gave a pale yellow solution, which was filtered and reduced to dryness in vacuo to leave a pale yellow solid. The solid was washed with diethyl ether (2 × 5 mL) to yield 2.8 g (45%) of product. ***CAUTION:*** *This compound is pyrophoric and will occasionally detonate upon exposure to air*. Diffusion of diethyl ether vapor into a benzene solution of **2** afforded pale yellow block-shaped crystals suitable for X-ray analysis. Absorption spectrum (benzene): λ_{max} (ϵ_M) 265 (sh, 31 200) nm. Absorption spectrum (MeCN): λ_{max} (ϵ_M) 290 (sh, 48 000) nm. IR (solid, ATR): ν_{CC} 2066 (m), ν_{CSi} 841 (s) cm^{-1}. ES$^-$-MS (MeCN): *m*/*z* 472 ([**2** − 4Li − 2CCSiMe$_3$ − 4C$_4$H$_{10}$O + Fe]$^{2-}$), 695 ([**2** − 4LiCCSiMe$_3$ − 4C$_4$H$_{10}$O + FeH]$^-$). Anal. Calcd for $C_{66}H_{130}FeLi_8O_4Si_{10}$: C, 57.44; H, 9.49. Found: C, 56.84; H, 9.84. ^{1}H NMR (CD_3CN): δ 3.40 (q, J_{HH} = 6.9 Hz, 16H; $(CH_3CH_2)_2O$), 1.11 (t, J_{HH} = 6.9 Hz, 24H; $(CH_3CH_2)_2O$), 0.13 (m, 90H; $Si(CH_3)_3$). ^{13}C{^{1}H} NMR (C_6D_6): δ 161, 135, 115, and 94.3 (s, Fe*CC*Si and Li*CC*Si); 66.5 (s, $(CH_3CH_2)_2O$); 15.7 (s, $(CH_3CH_2)_2O$); 2.27−0.83 (m, SiCH_3). This compound is soluble in polar and nonpolar solvents but decomposes in protic solvents such as methanol.

$Li_3[Co(CCSiMe_3)_6]\cdot 6THF$ (3). This compound was prepared by using $Co(CF_3SO_3)_2$ (1.0 g, 2.8 mmol) in a procedure directly analogous to that described above for compound **1**. After the reaction mixture was stirred for 10 h, the solution was filtered to remove unreacted $Co(CF_3SO_3)_2$ before the reaction was stored at −25 °C for 3 days. Yield: 231 mg (13%) of off-white solid. Pale yellow octahedron-shaped crystals suitable for X-ray analysis were grown by chilling a concentrated THF solution at −25 °C for two weeks. Absorption spectrum (hexanes): λ_{max} (ϵ_M) 201 (59 200), 244 (sh, 1964), 273 nm (sh, 1663). Absorption spectrum (MeCN): λ_{max} (ϵ_M) 267 (sh, 16 400), 328 (788) nm. IR (solid, ATR): ν_{CC} 1989 (m), ν_{CSi} 829 (s) cm^{-1}. The compound is diamagnetic. ES$^-$-MS (MeCN): *m*/*z* 643 ([**3** − 3Li − 6THF + 2H]$^-$), 655 ([**3** − Li − 6THF]$^-$). Anal. Calcd for $C_{54}H_{102}CoLi_3O_6Si_6$: C, 59.63; H, 9.38. Found: C, 57.78; H, 9.17. ^{1}H NMR (C_6D_6): δ 3.73 (br, 24H; $(CH_2CH_2)_2O$), 1.48 (br, 24H; $(CH_2CH_2)_2O$), 0.29 (s, 54H; SiCH_3). ^{13}C{^{1}H}-NMR (C_6D_6): δ 111 (s, Co*CC*Si), 68.9 (s, $(CH_2CH_2)_2O$), 26.1 (s, $(CH_2CH_2)_2O$), 3.38−1.52 (m, SiCH_3). This compound is soluble in polar and nonpolar solvents but decomposes in protic solvents such as methanol.

$Li_8[Cr_2O_4(CCSiMe_3)_6]\cdot 6LiCCSiMe_3\cdot 4glyme$ (4). This compound was prepared by using glyme in place of THF in a procedure directly analogous to that described above for compound **1**. Initially, no precipitate was obtained from the reaction. Upon standing at room temperature for 5 months, however, 135 mg (6%) of product formed as red block-shaped crystals. IR (solid, ATR): ν_{CC} 2006 (w), 1987 (w), ν_{CSi} 856 (m), 837 (m) cm^{-1}. ES$^+$-MS (MeCN:THF, 95:5): *m*/*z* 407 ([$CrO_4(CCSiMe_3)_3$]$^+$). Anal. Calcd for $C_{76}H_{148}Cr_2Li_{14}O_{12}Si_{12}$: C, 50.93; H, 8.32. Found: C, 50.68; H, 8.48.

$Li_3[Co(CCSiMe_3)_5(CCH)]\cdot LiCF_3SO_3\cdot 8THF$ (5). A solution of ^{n}BuLi (0.8 mL, 2.0 mmol, 2.5 M in hexane) was added to a solution of $HCCSiMe_3$ (0.32 mL, 2.3 mmol) in 8 mL of THF at −25 °C. After being stirred at room temperature for 1 h, the solution was cooled back to −25 °C and anhydrous $Co(CF_3SO_3)_2$ (0.20 g, 0.56 mmol) was added. Upon warming to room temperature and being stirred for 10 h, a dark brown solution formed. Following removal of the unreacted $Co(CF_3SO_3)_2$ by filtration, storage of the solution at −25 °C for 1 week afforded the product in approximately 20% yield as yellow block-shaped crystals suitable for X-ray analysis. Absorption spectrum (benzene): λ_{max} (ϵ_M) 250 (sh, 65 000). IR (solid, ATR): ν_{CC} 1996 (s), 1934 (w), ν_{CSi} 833 (s), ν_{CH} 3273 (w) cm^{-1}. The compound is diamagnetic. ^{1}H NMR ($CDCl_3$): δ 3.75 (br, 32H; $(CH_2CH_2)_2O$), 2.07 (s, 1H; ≡C*H*), 1.50 (br, 32H; $(CH_2CH_2)_2O$), 0.29 (s, 45H; SiCH_3).

X-Ray Structure Determinations. Single-crystal X-ray structure determinations were performed for compounds **1**−**5** (see Table 1). Crystals were quickly coated in Paratone-N oil under a nitrogen

atmosphere, mounted on glass fibers, transferred to a Siemens SMART diffractometer, and cooled in a dinitrogen stream. Initial lattice parameters were obtained from from a least-squares analysis of more than 30 centered reflections; these parameters were later refined against all data. A full hemisphere of data was collected for all compounds. Crystals of compounds **1** and **2** showed slight decay at the corners after data collection. Data were integrated and corrected for Lorentz polarization effects using SAINT and were corrected for absorption effects using SADABS 2.3.

Space group assignments were based upon systematic absences, *E* statistics, and successful refinement of the structures. Structures were solved by direct methods with the aid of successive difference Fourier maps and were refined against all data using the SHELXTL 5.0 software package. Thermal parameters for all non-hydrogen atoms were refined anisotropically, except the glyme solvate molecules in **4**. Hydrogen atoms were assigned to ideal positions and refined using a riding model with an isotropic thermal parameter 1.2 times that of the attached carbon atom (1.5 times for methyl hydrogens).

Other Physical Measurements. Absorption spectra were measured with a Hewlett-Packard 8453 spectrophotometer. Infrared spectra were recorded on a Nicolet Avatar 360 FTIR spectrometer equipped with a horizontal attenuated total reflectance (ATR) accessory. Cyclic voltammetry was performed in a 0.1 M solution of $(Bu_4N)PF_6$ in THF using a Bioanalytical systems CV-50W voltammograph, a platinum disk working electrode, a platinum wire supporting electrode, and a silver wire reference electrode. Reported potentials are all referenced to the $[FeCp_2]^{0/+}$ couple and were determined using ferrocene as an internal standard. Magnetic susceptibility data were measured on a Quantum Design MPMS-XL SQUID magnetometer. Mass spectrometric measurements were performed on VG Quattro (Micromass) spectrometer equipped with an analytical electrospray ion source instrument. NMR spectra were measured with a Bruker AVB 400 MHz instrument. Elemental analyses were performed by the UC Berkeley, Department of Chemistry Analytical Facility. These analyses were sometimes found to be unsatisfactory, particularly with regard to carbon content of the samples. This is not uncommon for acetylide-rich compounds and has been attributed to the extreme air sensitivity of the materials and/or the formation of metal carbides upon combustion.[17]

Electronic Structure Calculations. Density functional theory (DFT) calculations were performed using revision B.04 of Gaussian 03[26] with a spin-restricted formalism for compounds **2** and **3** and an unrestricted formalism for compound **1**; only negligible spin contamination was observed. Electronic structure calculations were performed on $[Cr(CCH)_6]^{3-}$, $[Fe(CCH)_6]$,$^{4-}$ and $[Co(CCH)_6]^{3-}$ as models for complexes **1**, **2**, and **3**.[17] Complex geometries were taken from the crystal structures of **1**, **2**, and **3** and then optimized using the B3LYP functional.[27] In all cases, the bond lengths for the optimized structures deviated from those observed in the crystal structure by less than 3%. Effective core potentials were employed for Cr, Co, and Fe (LanL2DZ), together with the corresponding Gaussian basis sets for C and H.[28] To address the negative overall charge of the complexes, basis sets were chosen that added diffuse and polarization functions to all non-hydrogen atoms, including the metal centers. Geometry optimizations performed in which the negative charge was compensated by employing a surrounding sphere of positive charge or by including Na^+ cations did not produce significantly different results, with the bond lengths in the optimized structure again deviating from those of the crystal structure by no more than 3%. TD-DFT calculations were performed using B3LYP/LanL2DZ and the geometry-optimized DFT ground-states as an initial reference.[29]

Results and Discussion

Syntheses. We had previously found that $LiCCSiMe_3$ can serve as a suitable reagent for the preparation of complexes such as $[(Me_3tacn)Cr(CCSiMe_3)_3]$ (Me_3tacn = *N*,*N*,*N*-trimethyl-1,4,7-triazacyclononane).[30] Our initial attempts to use an analogous procedure in synthesizing a hexaacetylide complex of chromium(III) employed $CrCl_3 \cdot 3THF$;[31] however, in a variety of ethereal solvents, only intractable mixtures were obtained. We therefore turned to use of anhydrous $CrCl_2$, following the precedent set by the synthesis of compounds such as $Li_3[CrPh_6]$.[32] Under a dinitrogen atmosphere, a solution of $LiCCSiMe_3$ was generated by adding ^{n}BuLi to a solution of $HCCSiMe_3$ in THF at −25 °C. Addition of $CrCl_2$ followed by stirring at room temperature for 10 h then gave a dark orange solution containing the hexaacetylide complex, which, upon rechilling at −25 °C, yielded microcrystalline $Li_3[Cr(CCSiMe_3)_6] \cdot 6THF$ (**1**). Magnetic susceptibility measurements showed the compound to possess a magnetic moment of 3.85 μ_B at 295 K, consistent with the presence of an $S = {}^3/_2$ chromium(III) complex. When the analogous reaction between $CrCl_2$ and $LiCCSiMe_3$ was performed in glyme solution, the enhanced solubility of compound **1** in glyme prohibited its isolation without coprecipitation of a multitude of side-products. Leaving this reaction solution to stand for five months, however, afforded large, red, block-shaped crystals of $Li_8[Cr_2O_4(CCSiMe_3)_6] \cdot 6LiCCSiMe_3 \cdot 4glyme$ (**4**) exclusively.

The analogous hexaacetylide complex of iron(II) was readily accessed by extension of the foregoing approach. Here, the reaction is best performed using $Fe(CF_3SO_3)_2 \cdot$

(26) Frisch, M. J.; Trucks, G. W.; Schlegel, H. B.; Scuseria, G. E.; Robb, M. A.; Cheeseman, J. R.; Montgomery, J. A., Jr.; Vreven, T.; Kudin, K. N.; Burant, J. C.; Millam, J. M.; Iyengar, S. S.; Tomasi, J.; Barone, V.; Mennucci, B.; Cossi, M.; Scalmani, G.; Rega, N.; Petersson, G. A.; Nakatsuji, H.; Hada, M.; Ehara, M.; Toyota, K.; Fukuda, R.; Hasegawa, J.; Ishida, M.; Nakajima, T.; Honda, Y.; Kitao, O.; Nakai, H.; Klene, M.; Li, X.; Knox, J. E.; Hratchian, H. P.; Cross, J. B.; Bakken, V.; Adamo, C.; Jaramillo, J.; Gomperts, R.; Stratmann, R. E.; Yazyev, O.; Austin, A. J.; Cammi, R.; Pomelli, C.; Ochterski, J. W.; Ayala, P. Y.; Morokuma, K.; Voth, G. A.; Salvador, P.; Dannenberg, J. J.; Zakrzewski, V. G.; Dapprich, S.; Daniels, A. D.; Strain, M. C.; Farkas, O.; Malick, D. K.; Rabuck, A. D.; Raghavachari, K.; Foresman, J. B.; Ortiz, J. V.; Cui, Q.; Baboul, A. G.; Clifford, S.; Cioslowski, J.; Stefanov, B. B.; Liu, G.; Liashenko, A.; Piskorz, P.; Komaromi, I.; Martin, R. L.; Fox, D. J.; Keith, T.; Al-Laham, M. A.; Peng, C. Y.; Nanayakkara, A.; Challacombe, M.; Gill, P. M. W.; Johnson, B.; Chen, W.; Wong, M. W.; Gonzalez, C.; Pople, J. A. *Gaussian 03*, revision B.04; Gaussian, Inc.: Wallingford, CT, 2004.

(27) Zheng, K. C.; Wang, J. P.; Peng, W. L.; Liu, X. W.; Yun, F. C. *J. Phys. Chem. A* **2001**, *105*, 10899.

(28) (a) Hay, P. J.; Wadt, W. R. *J. Chem. Phys.* **1985**, *82*, 270. (b) Wadt, W. R.; Hay, P. J. *J. Chem. Phys.* **1985**, *82*, 284. (c) Hay, P. J.; Wadt, W. R. *J. Chem. Phys.* **1985**, *82*, 299. (d) Dunning, T. H., Jr.; Hay, P. J. In *Modern Theoretical Chemistry*; Schaefer, H. F., Ed.; Plenum: New York, 1976; Vol. 3, p 1. (e) Check, C. E.; Faust, T. O.; Bailey, J. M.; Wright, B. J.; Gilbert, T. M.; Sunderlin, L. S. *J. Phys. Chem. A* **2001**, *105*, 8111.

(29) (a) Stratmann, R. E.; Scuseria, G. E.; Frisch, M. J. *J. Chem. Phys.* **1998**, *8218*, 109. (b) Bauernschmitt, R.; Ahlrichs, R. *Chem. Phys. Lett.* **1996**, *454*, 256. (c) Casida, M. E.; Jamorski, C.; Casida, K. C.; Salahub, D. R. *J. Chem. Phys.* **1998**, *108*, 4439.

(30) Berben, L. A.; Long, J. R. *J. Am. Chem. Soc.* **2002**, *124*, 11588.

(31) Shamir, J. *Inorg. Chim. Acta* **1989**, *156*, 163.

(32) Olmstead, M. M.; Power, P. P.; Shoner, S. C. *Organometallics* **1988**, *7*, 1380.

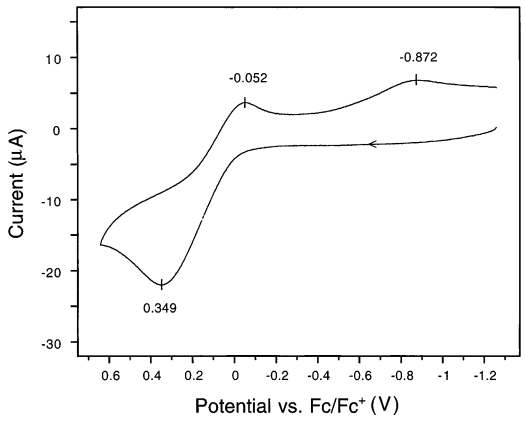

Figure 1. Cyclic voltammogram of a 0.20 mM solution of **2** in THF scanned at 1000 mV/s.

MeCN in diethyl ether and generates $Li_4[Fe(CCSiMe_3)_6]\cdot 4LiCCSiMe_3\cdot 4Et_2O$ (**2**) in 45% yield as a pale yellow solid. Efforts to prepare $Li_4[Fe(CCSiMe_3)_6]$ without incorporating an excess of $LiCCSiMe_3$ simply resulted in lower yields of **2**. The $^{13}C\{^1H\}$-NMR spectrum of **2** in C_6D_6 displays four signals between 94.3 and 161 ppm, corresponding to the four unique acetylenic carbon atoms (two each belonging to the Fe−C≡C−$SiMe_3$ and Li−C≡C−$SiMe_3$ moieties). Thus, each type of acetylide ligand is present in the same average environment. Figure 1 depicts the cyclic voltammogram obtained for a THF solution of **2** scanned at 1000 mV/s. An oxidation wave attributed to formation of $[Fe(CCSiMe_3)_6]^{3-}$ is apparent at $E = +0.349$ V versus $[FeCp_2]^{0/1+}$. This species decomposes, giving rise to the reduction peak at −0.872 V; however, at fast scan rates, a return wave presumably associated with regeneration of $[Fe(CCSiMe_3)_6]^{4-}$ appears at −0.052 V.

A related reaction employing $Co(CF_3SO_3)_2$ in THF afforded $Li_3[Co(CCSiMe_3)_6]\cdot 6THF$ (**3**) as an off-white solid in 13% yield. The low yield is attributed in part to the limited solubility of $Co(CF_3SO_3)_2$ in THF. Use of additional $Co(CF_3SO_3)_2$ in the reaction, however, led to formation of the heteroleptic compound $Li_3[Co(CCSiMe_3)_5(CCH)]\cdot LiCF_3SO_3\cdot 8THF$ (**5**) instead of **3**. Possibly, the deprotection of a trimethylsilylacetylide ligand during the reaction is connected to the oxidation of the cobalt center, such that an excess of the ligand is required to obtain the homoleptic complex via substitution. The $^{13}C\{^1H\}$-NMR spectrum of **3** in C_6D_6 displays a single resonance at 111 ppm, corresponding to just one of the carbon atoms within the Co−C≡C−$SiMe_3$ moieties. The other quaternary carbon resonance could not be identified; however, this is not uncommon for the ^{13}C NMR spectra of such species.[33]

Crystal Structures. The structures of compounds **1**−**3** were determined by single-crystal X-ray analysis. While **1** and **3** are isostructural and crystallize in space group $Pa\bar{3}$, **2** crystallizes in the lower-symmetry space group $P2_1/c$. Within these crystals, each homoleptic trimethylsilylacetylide complex displays a quite regular octahedral coordination at the metal center (see Figure 2), with C−M−C angles deviating from 90° by no more than a few degrees. Selected interatomic distances and angles are listed in Table 2. The mean M−C distances of 2.077, 1.930(9), and 1.908 Å for M = Cr^{III}, Fe^{II}, and Co^{III}, respectively, are nearly identical to those observed in the potassium salts of the analogous hexacyanometalate complexes: 2.08(2), 1.92(5), and 1.89(2) Å.[34] The C−C separations in **1**−**3**, which vary between 1.212(5) and 1.251(8) Å, are slightly longer than the 1.2033(2) Å distance in acetylene[35] and fall between the median and the high end of bond lengths for metal−alkynyl complexes.[18] In keeping with the expected triple-bond character of the $C\equiv C^{2-}$ unit, the M−C≡C angles are all quite linear, falling within the range 173.9(5)−178.7(3)°. The somewhat bent C≡C−Si angles of 162.9(2)° and 159.4(4)° in the structures of **1** and **3**, respectively, are attributed to steric crowding by the $[Li(THF)_2]^+$ moieties coordinated in a side-on fashion between alternating pairs of trimethylsilylacetylide ligands (see Figure 3). In contrast, Figure 4 shows that the Li^+ cations and accompanying Et_2O molecules and Me_3SiCC^- anions surround the $[Fe(CCSiMe_3)_6]^{4-}$ complex in **2** in a more isotropic manner, resulting in a more linear mean C≡C−Si angle of 171(3)°. To our knowledge, these represent the first structurally characterized examples of hexaacetylide complexes of first-row transition metal ions.

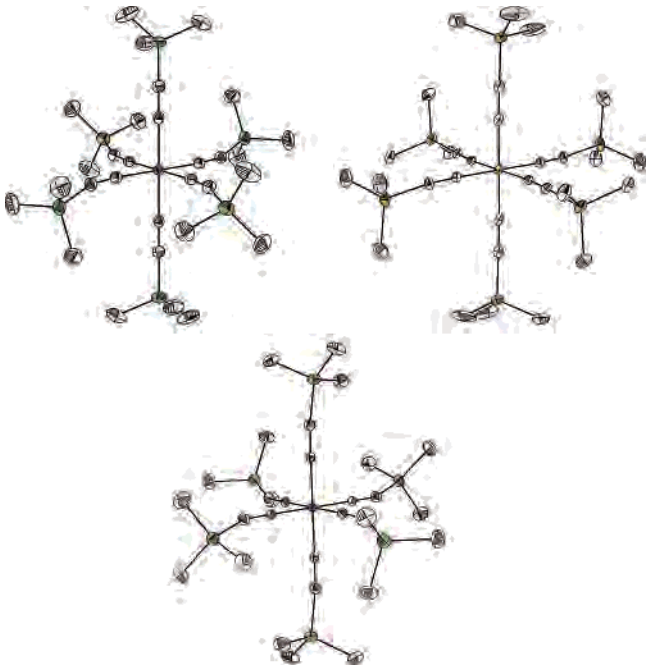

Figure 2. Structures of the octahedral complexes $[Cr(CCSiMe_3)_6]^{3-}$ (left), $[Fe(CCSiMe_3)_6]^{4-}$ (right), and $[Co(CCSiMe_3)_6]^{3-}$ (below) in **1**, **2**, and **3**, respectively. Ellipsoids are drawn at the 30% probability level, and H atoms are omitted for clarity. Pink, yellow, blue, green, and gray ellipsoids represent Cr, Fe, Co, Si, and C atoms, respectively. The chromium and cobalt complexes reside on a $\bar{3}$ site in the crystal, while the iron complex resides on a crystallographic inversion center.

(33) Silverstein, R. M.; Bassler, G. C.; Morrill, T. C. *Spectrometric Identification of Organic Compounds*, 5th ed.; John Wiley and Sons: New York, 1991; p 232.

(34) (a) Jagner, S.; Ljungström, E.; Vannerberg, N.-G. *Acta Chem. Scand.* **1974**, *A28*, 623. (b) Pospelov, V. A.; Zhdanov, G. S. *Zh. Fiz. Khim.* **1947**, *21*, 879. (c) Reynhardt, E. C.; Boeyens, J. C. A. *Acta Crystallogr.* **1972**, *B28*, 524.

(35) Fast, H.; Welsh, H. L. *J. Mol. Spectrosc.* **1972**, *41*, 203.

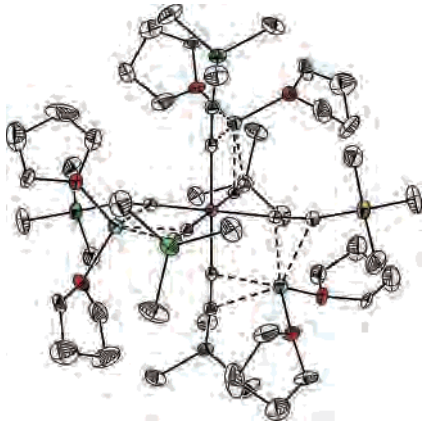

Figure 3. Structure of **1**, showing the arrangement of Li^+ cations and THF solvate molecules around the $[Cr(CCSiMe_3)_6]^{3-}$ complex. Pink, green, gray, red, and light blue ellipsoids represent Cr, Si, C, O, and Li atoms, respectively; H atoms are omitted for clarity. Selected interatomic distances (Å): Li−C, 2.257(9)−2.597(9); Li−O, 1.959(9).

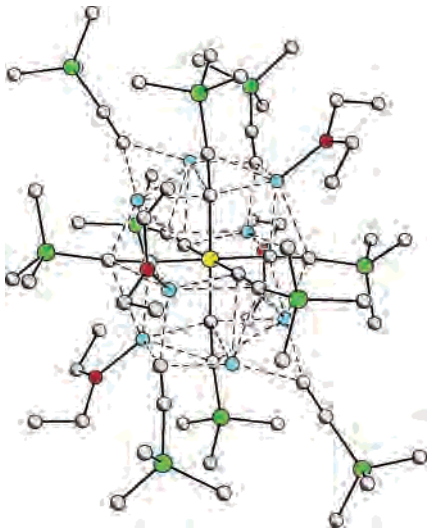

Figure 4. Structure of **2**, showing the arrangement of Li^+ cations, $MeSi_3CC^-$ anions, and diethyl ether solvate molecules around the $[Fe(CCSiMe_3)_6]^{4-}$ complex. Yellow, green, gray, red, and light blue spheres represent Fe, Si, C, O, and Li atoms, respectively; H atoms are omitted for clarity. Selected interatomic distances (Å): Li−C, 2.11(1)−2.72(1), Li−O, 1.97(1).

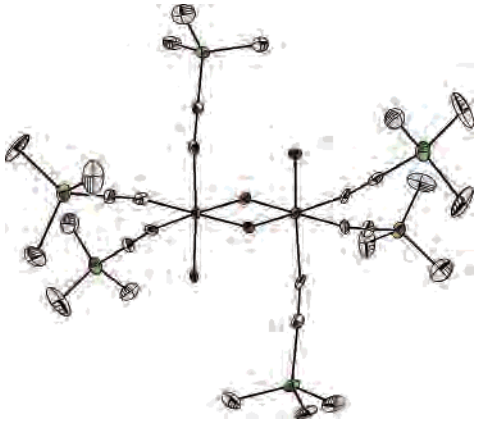

Figure 5. Structure of the oxo-bridged complex $[Cr_2O_4(CCSiMe_3)_6]^{8-}$ in **4**. Pink, green, gray, and red ellipsoids represent Cr, Si, C, and O atoms, respectively; H atoms are omitted for clarity. The complex resides on a crystallographic inversion center. Selected mean interatomic distances (Å) and angles (deg): $Cr-O_{terminal}$, 1.94(3); $Cr-O_{bridging}$, 2.05(3); Cr−C, 2.12(3); C≡C, 1.23(4); Cr−O−Cr, 94.7(5); O−Cr−O, 85(2); C−Cr−C, 89.1(8); Cr−C≡C, 171(2); Si−C≡C, 177(2).

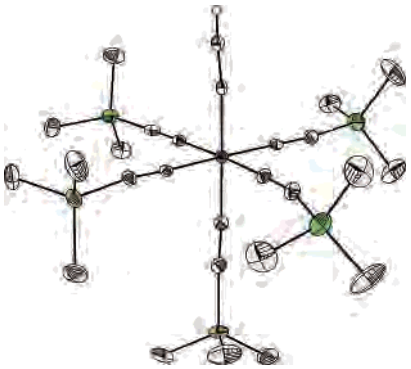

Figure 6. Structure of the $[Co(CCSiMe_3)_5(CCH)]^{3-}$ complex in **5**. Blue, green, and gray ellipsoids represent Co, Si, and C atoms, respectively; ellipsoids are drawn at the 30% probability level. The small white sphere represents a H atom; H atoms on the methyl groups are omitted for clarity.

As depicted in Figure 5, the crystal structure of **4** features a binuclear complex of formula $[Cr_2O_4(CCSiMe_3)_6]^{8-}$. Therein, two Cr^{III} centers, separated by a distance of 3.014 Å, are bridged symmetrically through two oxo ligands with a Cr−O−Cr angle of 94.7(5)°. In addition, each chromium atom is ligated by a terminal oxo atom and three trimethylsilylacetylide groups, resulting in an octahedral coordination environment. The Cr−C, C≡C, and C−Si distances of 2.12(3), 1.23(4), and 1.84(4) Å, respectively, are very similar to those in **1** (see Table 2). Fourteen Li^+ cations are bound to the acetylide ligands in a side-on fashion (see Figure S2 in the Supporting Information). Coordinated to these cations are four glyme solvate molecules and six additional trimethylsilylacetylide anions. To our knowledge, this molecule represents the first structurally characterized complex bearing a $(Cr{=}O)_2(\mu\text{-}O)_2$ moiety with octahedral coordination of the chromium(III) centers.

The crystal structure of **5** contains an octahedral cobalt complex (see Figure 6) bearing five trimethylsilylacetylide ligands and another ligand, the nature of which, C_2H^-, N_2, or O_2^{2-}, could not be definitively established via crystallography. As indicated in Table 2, the observed bond lengths and angles are in close agreement with those of $[Co(CCSiMe_3)_6]^{3-}$, with the exception of the C≡C−Si angles. Further characterization showed compound **5** to be diamagnetic,

Table 2. Selected Interatomic Distances (Å) and Angles (deg) for the Hexaacetylide Complexes in **1**−**3** and **5**

	$[Cr(CCSiMe_3)_6]^{3-}$	$[Fe(CCSiMe_3)_6]^{4-}$	$[Co(CCSiMe_3)_6]^{3-}$	$[Co(CCSiMe_3)_5(CCH)]^{3-}$
M−C	2.077(3)	1.917(7)−1.935(7)	1.908(3)	1.90(1)
C≡C	1.215(4)	1.233(8)−1.251(8)	1.212(5)	1.23(1)
C−Si	1.824(3)	1.831(8)−1.856(7)	1.823(4)	1.818(9)
C−M−C	87.76(9)−92.24(9)	86.7(2)−92.1(2)	87.9(2)−92.1(2)	87.1(9)−91.3(5)
M−C≡C	175.2(2)	173.9(5)−176.3(6)	178.7(3)	176.8(8)
C≡C−Si	162.9(2)	169.2(5)−175.3(5)	159.4(4)	171(4)

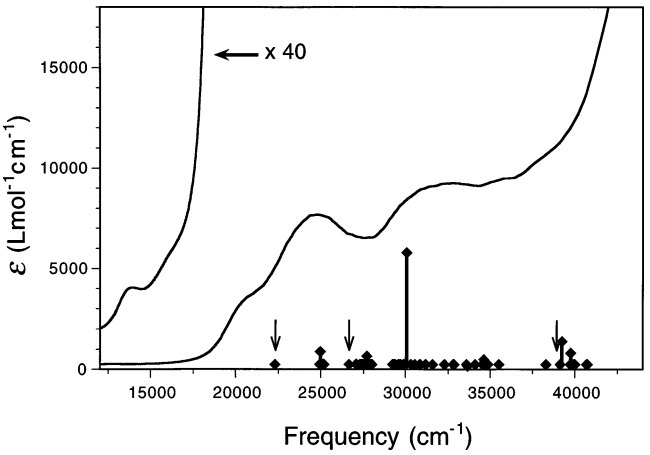

Figure 7. Electronic absorption spectrum for a solution of **1** in hexanes compared with the results of TD-DFT calculations performed on $[Cr(CCH)_6]^{3-}$. The calculated spectrum has been shifted by +6670 cm^{-1}, as explained in the text. Arrows denote the positions of d−d transitions.

indicating that cobalt is present in the +3 oxidation state and, hence, the ligand must possess a uninegative charge. The identity of the ligand as acetylide, C_2H^-, was confirmed by infrared spectroscopy (ν_{CH} = 3273 cm^{-1}) and ^1H NMR spectroscopy.

Electronic Absorption Spectra. Compounds **1**−**3** provided an opportunity for probing the nature of the ligand field presented by acetylide-type ligands via UV−visible absorption spectroscopy. Figure 7 displays the electronic absorption spectrum observed for a solution of **1** in hexanes. Peak positions and amplitudes were determined by fitting Gaussian curves to the spectrum using IGOR Pro 4.0 (see Figure S3 in the Supporting Information). In **1**, the t_{2g}^3 electron configuration of $[Cr(CCSiMe_3)_6]^{3-}$ lends itself to the presence of both MLCT and LMCT transitions. Accordingly, the high-energy, high-intensity transitions at 43 900, 32 900, and 24 800 cm^{-1} are assigned as charge-transfer bands, most likely an LMCT and two MLCT transitions, respectively. Consistent with these assignments, the bands display vibrational fine structure in spectra collected in acetonitrile solution. Lower-intensity bands appear as shoulders on the tails of the charge-transfer bands, occurring at 20 200, 16 200, 13 800, and 13 300 cm^{-1} (see Table 3). The somewhat inflated extinction coefficient associated with each of these transitions is likely due to a combination of three factors: intensity stealing from a proximal charge-transfer band,[36] the somewhat covalent nature of the metal−acetylide bond, and the less-than-perfect O_h symmetry. This last factor can be expected to arise owing to ion pairing with the Li^+ countercations and associated solvate molecules (as, for example, in the solid-state structure depicted in Figure 3), rendering the transitions only incompletely Laporte forbidden. With an extinction coefficient of 1110 L/mol·cm, the peak at 20 200 cm^{-1} is assigned as the spin-allowed $d-d$ transition $^4T_{2g} \leftarrow {}^4A_{2g}$. The much weaker, lower-energy bands at 16 200 (18), 13 800 (12), and 13 300 cm^{-1} (16 L/mol·cm) are assigned as spin-forbidden transitions to the $^2T_{2g}$, $^2T_{1g}$, and ^2E_g states, respectively. Taken together, these results

(36) Fenske, R. F. *J. Am. Chem. Soc.* **1967**, *89*, 252.

Table 3. Observed and Calculated d−d Absorption Bands for Trimethylsilylacetylide Complexes of Chromium(III), Iron(II), and Cobalt(III)

complex	energy (cm^{-1})[a]	ϵ (L/mol·cm)[b]	assignment
$[Cr(CCSiMe_3)_6]^{3-}$	24 810		$^4T_{1g} \leftarrow {}^4A_{1g}$
	20 240	1110	$^4T_{2g} \leftarrow {}^4A_{1g}$
	16 200	18	$^2T_{2g} \leftarrow {}^4A_{1g}$
	13 800	12	$^2T_{1g} \leftarrow {}^4A_{1g}$
	13 300	16	$^2E_g \leftarrow {}^4A_{1g}$
$[Fe(CCSiMe_3)_6]^{4-}$	54 050		$^1T_{2g} \leftarrow {}^1A_{1g}$
	53 190		$^1T_{2g} \leftarrow {}^1A_{1g}$
	36 900		$^1T_{2g}(D) \leftarrow {}^1A_{1g}$
	31 150		$^1T_{1g} \leftarrow {}^1A_{1g}$
$[Co(CCSiMe_3)_6]^{3-}$	58 140		$^1E_g \leftarrow {}^1A_{1g}$
	54 350		$^1T_{2g} \leftarrow {}^1A_{1g}$
	36 900		$^1T_{2g}(D) \leftarrow {}^1A_{1g}$
	30 500	788	$^1T_{1g} \leftarrow {}^1A_{1g}$

[a] Entries in bold-face type were extracted from the observed UV−vis spectrum, while the other entries correspond to peak positions calculated using TD-DFT. [b] Values are taken from experimental data.

Table 4. Ligand Field Parameters for Trimethylsilylacetylide and Cyanide Complexes of Chromim(III), Iron(II), and Cobalt(III)[27]

complex	Δ_o (cm^{-1})	$B_{complex}$	$B_{free\ ion}$	β
$[Cr(CCSiMe_3)_6]^{3-}$	20 200	530	845	0.544
$[Fe(CCSiMe_3)_6]^{4-}$	32 450	457	830	0.550
$[Co(CCSiMe_3)_6]^{3-}$	32 500	516	1100	0.469
$[Cr(CN)_6]^{3-}$	26 300	520	845	0.560
$[Fe(CN)_6]^{4-}$	33 000	380	830	0.458
$[Co(CN)_6]^{3-}$	34 000	430	1100	0.390

yield an estimate for the value of the ligand field splitting parameter, Δ_o = 20 200 cm^{-1}, and for the Racah parameter, B = 530 cm^{-1} (see Table 4). This places trimethylsilylacetylide between chloride (Δ_o = 18 700 cm^{-1})[37] and methyl (Δ_o = 20 800 cm^{-1}),[38] and well before cyanide (Δ_o = 26 600 cm^{-1}),[39] in the spectrochemical series for chromium(III).[40] Given the nearly equal positions of the lowest-energy absorption bands of 22 000 and 22 300 cm^{-1}, observed for $[(Me_3tacn)Cr(CCH)_3]$ and $[(Me_3tacn)Cr(CCSiMe_3)_3]$, respectively,[30] a very similar ligand field strength can be anticipated for the unsubstituted acetylide ligand itself.

The reduction of B to 530 cm^{-1} from the free-ion value[41] of 918 cm^{-1} for Cr^{3+} demonstrates a strong nephelauxetic effect by the trimethylsilylacetylide ligand. This indicates significant delocalization of the d electrons within the complex, which is attributable to strong covalency and/or substantial π-bonding interactions between the metal center and its ligands.[40] Ligands with a nephelauxetic effect of similar magnitude include the π-acceptor cyanide (B = 520 cm^{-1}), and the π-donor chloride (B = 510 cm^{-1}). From the small value of Δ_o for $[Cr(CCSiMe)_6]^{3-}$, we can conclude that the interaction in the case of trimethylsilylacetylide is π-donor in character. Indeed, as discussed below, DFT calculations performed on $[Cr(CCH)_6]^{3-}$ show its frontier

(37) Hatfield, W. E.; Fay, R. C.; Pfluger, C. E.; Piper, T. S. *J. Am. Chem. Soc.* **1963**, *85*, 265.
(38) Bohmer, W.-H.; Majeda, K.; Kurras, E.; Rosenthal, U. *Z. Anorg. Chem.* **1979**, *458*, 69.
(39) Alexander, J. J.; Gray, H. B. *J. Am. Chem. Soc.* **1968**, *90*, 4260.
(40) Lever, A. B. P. *Inorganic Electronic Spectroscopy*, 2nd ed.; Elsevier: Amsterdam, 1984.
(41) Bersuker, I. B.; *Electronic Structure and Properties of Transition Metal Compounds*; Wiley-Interscience: New York, 1996.

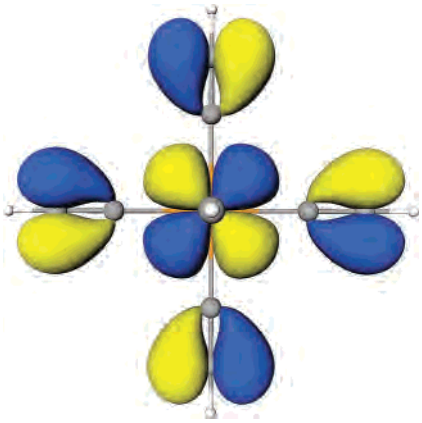

Figure 8. Depiction of one of the t_{2g} HOMOs of $[Cr(CCH)_6]^{3-}$, as calculated using DFT.

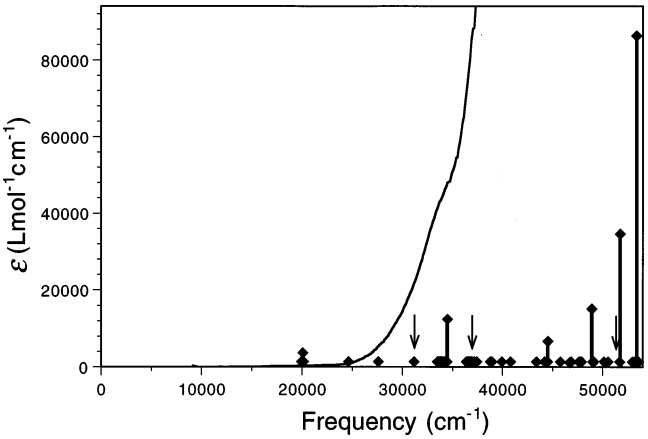

Figure 9. Electronic absorption spectrum for a solution of **2** in acetonitrile compared with the results of TD-DFT calculations performed on $[Fe(CCH)_6]^{4-}$. The calculated spectrum has been shifted by -7270 cm^{-1}, as explained in the text. Arrows denote the d−d transitions.

t_{2g} orbitals to be Cr−C π-antibonding in character, owing to contributions from the alkynyl π-bonding orbitals (see Figure 8).

The electronic absorption spectra of $[Fe(CCSiMe_3)_6]^{4-}$ and $[Co(CCSiMe_3)_6]^{3-}$ in acetonitrile solution are dominated by intense charge-transfer bands that obscure the d−d transitions (see Figures 9 and 10). The lowest-energy shoulders in these spectra occur at 34 500 and 36 000 cm^{-1}. Given the extinction coefficients of 48 000 and 16 400 L/mol·cm, respectively, the corresponding transitions were assigned as LLCT or MLCT bands. Since both complexes have a t_{2g}^6 electron configuration, the presence of LMCT transitions this low in energy is unlikely. Furthermore, the intense bands upon whose tails these shoulders reside, are attributed to LLCT transitions. In addition, the UV−vis spectrum for $[Co(CCSiMe_3)_6]^{3-}$ features a well-resolved peak at 30 500 cm^{-1}, corresponding to the $^1T_{1g} \leftarrow {}^1A_{1g}$ transition. Further assignments for both of these complexes calibrated to these benchmarks could be achieved using the results of TD-DFT calculations, as discussed below.

Electronic Structure Calculations and Comparisons with Observed Spectra. As a complement to the spectroscopic measurements, electronic structure calculations were performed on $[Cr(CCH)_6]^{3-}$, $[Fe(CCH)_6]$,$^{4-}$ and $[Co(CCH)_6]^{3-}$

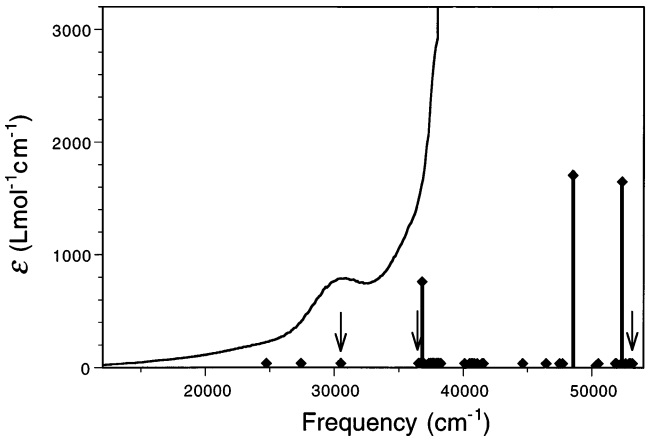

Figure 10. Electronic absorption spectrum for a solution of **3** in acetonitrile compared with the results of TD-DFT calculations performed on $[Co(CCH)_6]^{3-}$. The calculated spectrum has been shifted by -1960 cm^{-1}, as explained in the text. Arrows denote the d−d transitions.

model complexes. Initially, DFT calculations were performed on the ground-state configuration of each complex. In each case, a group of triply degenerate ligand-based molecular orbitals of symmetry, t_{1u}, t_{1g}, and t_{2u}, are located within 0.584, 2.05, and 0.490 eV below the HOMO for Cr^{III}, Fe^{II}, and Co^{III}, respectively. As illustrated in Figure 8, the HOMOs, a set of metal-based t_{2g} orbitals, are M−C π-antibonding in character owing to contributions from the acetylide π-bonding orbitals. The nature of this orbital interaction is in agreement with the results reported by Lichtenberger and co-workers, from photoelectron spectra measured on $Cp(CO)_2Fe(CCH)$, which showed that the metal−ligand filled−filled interactions predominate in the bonding scheme.[19]

TD-DFT calculations performed after the ground-state calculations yielded models which could be used to consolidate and extend the conclusions drawn from the UV−visible absorption spectra. Such calculations provide information about transitions in the absorption spectra, through evaluation of the characters, energies, and oscillator strengths of triplet and singlet excited states. Applications of TD-DFT to open-shell molecules are limited, and there is some debate as to whether the method is reliable for such systems. Several recent studies, however, have shown favorable comparisons between calculated and experimental spectra,[42] and so we have chosen to include the results from calculations performed on $[Cr(CCH)_6]^{3-}$ in the present discussion.

In the initial examination of the TD-DFT results, the calculated d−d absorption bands for each complex were compared with the experimental spectra to determine the energy by which they differed. Even neglecting the inadequacies associated with using perfectly octahedral complexes with acetylide in place of trimethylsilylacetylide, such difference are expected, owing to solvent effects and calculation inaccuracies. The solvent dependence of charge-

(42) For example: (a) Broclawik, E.; Borowski, T. *Chem. Phys. Lett.* **2001**, *339*, 433. (b) Ricciardi, G.; Rosa, A.; Baerends, E. J.; van Gisbergen, S. A. J. *J. Am. Chem. Soc.* **2002**, *124*, 12319. (c) Frolova, Y. V.; Avdeev, V. I.; Ruzankin, S. P.; Zhidomirov, G. M.; Fedotov, M. A.; Sadykov, V. A. *J. Phys. Chem. B* **2004**, *108*, 6969. (d) Machura, B. *Polyhedron* **2004**, *23*, 2363. (e) Wang, F.; Ziegler, T. *Mol. Phys.* **2004**, *102*, 2585.

transfer transitions, observed experimentally by us, and theoretically by others,[43] helps emphasize the importance of these effects. For $[Cr(CCH)_6]^{3-}$, the calculated spectrum is shifted to higher energy than observed by experiment, by 0.827 eV. A shift of this magnitude to higher energy is commonly observed in TD-DFT calculations employing the B3LYP functional due to overestimation of the HOMO−LUMO gap in calculations.[44] In the cases of $[Fe(CCH)_6]^{4-}$ and $[Co(CCH)_6]^{3-}$, the calculated absorption energies fall 0.901 and 0.243 eV below those observed by experiment.[45] Each calculated spectrum comprises a complicated manifold of transitions: in most cases, more than a single one-electron transition contributes to any given optical transition. Due to the O_h symmetry enforced upon the model complexes, only 18−24 of the 150 singlet and 50 triplet excited states calculated possess a nonzero oscillator strength. All d−d transitions are of course forbidden under O_h symmetry, and transitions to triplet states are spin-forbidden. However, these results do not reflect the complete picture, since neither vibronic coupling, intensity stealing, nor spin−orbit coupling are accounted for in the calculations. In addition, the true symmetry of the complexes is likely lower than O_h, owing to the Li^+ cations and solvate molecules bound within the ligand framework. Hence, it is hardly surprising that many of the calculated transitions with $f = 0$ are observed experimentally.

Employing $[Cr(CCH)_6]^{3-}$ as a model for $[Cr(CCSiMe_3)_6]^{3-}$, transition energies and assignments could be determined; however, due to the existence of a quartet ground state, the multiplicities of the excited states could not be extracted with complete certainty. The calculated excited-state manifold exhibits a series of charge-transfer transitions spanning the range 23040−37740 cm^{-1} (see Figure 7 and Table 5). As listed in Table 3, at lower energies, the two spin-allowed d−d transitions, $^4T_{1g} \leftarrow {}^4A_{2g}$ and $^4T_{2g} \leftarrow {}^4A_{2g}$, occur at a spacing of 0.541 eV apart. The coincidence of the experimentally observed $^4T_{2g} \leftarrow {}^4A_{2g}$ band with MLCT and LLCT transitions may help explain the inflated extinction coefficient of 1110 L/mol·cm observed for this transition.

The experimental UV−visible absorption spectrum of $[Fe(CCSiMe_3)_6]^{4-}$ displayed only a high-intensity charge-transfer band with a tail and shoulder extending into the visible region and obscuring all d−d transitions. An identical pattern was observed by TD-DFT and allowed the manifold of bands comprising the tail to be assigned as five LLCT and one MLCT transitions overlapping between 34 500 and 53 190 cm^{-1} (see Figure 9 and Table 5). By aligning the lowest in energy of the calculated LLCT bands with the experimentally observed shoulder at 290 nm, the positions of the d−d transitions and, hence, the approximate ligand field parameters of the complex could be inferred.[46] As enumerated in Table 3, transitions at 31 150, 36 900, 53 190, and 54 050 cm^{-1} were assigned as the $^1T_{1g} \leftarrow {}^1A_{1g}$, $^1T_{2g}(D) \leftarrow {}^1A_{1g}$, $^1T_{2g} \leftarrow {}^1A_{1g}$, and $^1E_g \leftarrow {}^1A_{1g}$ transitions, respectively. This permits estimation of the ligand field parameters as $\Delta_o = 32\,450$ cm^{-1} and $B = 457$ cm^{-1} (see Table 4), placing trimethylsilylacetylide between $-CNO^-$ ($\Delta_o = 27\,000$ cm^{-1})[47] and cyanide ($\Delta_o = 33\,000$ cm^{-1}) in the spectrochemical series for iron(II).[48]

Table 5. Calculated Charge-Transfer Absorption Bands for Trimethylsilylacetylide Complexes of Chromium(III), Iron(II), and Cobalt(III)

compound	excitation energy (cm^{-1})	f	assignment
$[Cr(CCH)_6]^{3-}$	23 040	0.0088	MLCT
	25 130	0.0013	LLCT/LMCT
	25 770	0.0061	LLCT/LMCT
	31 650	0.0001	LLCT
	32 680	0.0039	LLCT/LMCT
	34 840	0.0687	LLCT/MLCT
	37 310	0.0149	LLCT
	37 740	0.0079	LLCT/LMCT
$[Fe(CCH)_6]^{4-}$	20 040	0.0062	MLCT/LLCT
	34 500	0.0257	LLCT
	44 440	0.0013	LLCT
	46 730	0.0007	LLCT
	48 780	0.0318	LLCT
	51 810	0.0753	LLCT
$[Co(CCH)_6]^{3-}$	36 820	0.0394	MLCT
	48 540	0.0897	LMCT
	52 360	0.0867	LLCT
	54 640	0.0008	LLCT

TD-DFT and experimental results for $[Co(C{\equiv}CSiMe_3)_6]^{3-}$ also feature the tail of an intense charge-transfer band at high energy (see Figure 10). In this case, the tail is comprised of one LMCT, one MLCT, and two LLCT transitions spanning the range 36 820−58 480 cm^{-1}. As discussed previously, the lowest-energy d−d transition, $^1T_{1g} \leftarrow {}^1A_{1g}$, was observed experimentally as a shoulder located at 30 500 cm^{-1}. Further examination of the TD-DFT results predicts the remaining transitions, $^1T_{2g}(D) \leftarrow {}^1A_{1g}$, $^1T_{2g} \leftarrow {}^1A_{1g}$, and $^1E_g \leftarrow {}^1A_{1g}$, to occur at 36 900, 53 190, and 54 050 cm^{-1}, respectively. Hence, the ligand field splitting energy for $[Co(CCSiMe_3)_6]^{3-}$ can be estimated as $\Delta_o = 32\,450$ cm^{-1} and the Racah parameter as $B = 457$ cm^{-1}, consistent once more with significant π interaction between ligand and metal center. This places trimethylsilylacetylide between $-CNO^-$ ($\Delta_o = 26\,100$ cm^{-1})[47] and $P(OCH_2)_3CMe$ ($\Delta_o = 33\,200$ cm^{-1})[49] in the spectrochemical series for cobalt(III). Thus, once again, the results indicate that the acetylide ligand is of weaker field strength than cyanide ($\Delta_o = 34\,500$ cm^{-1})[39] and has a significant π overlap with the metal d orbitals, most likely of a π-donor nature.

Outlook

The foregoing results demonstrate the feasibility of synthesizing soluble homoleptic acetylide-type complexes of

(43) Hummel, P.; Oxgaard, J.; Goddard, W. A.; Gray, H. B. *Inorg. Chem.* **2005**, *44*, 2454.
(44) Monat, J. E.; Rodriguez, J. H.; McCusker, J. K. *J. Phys. Chem. A* **2002**, *106*, 7399 and references therein.
(45) For comparison, TD-DFT calculations were tested on known hexachloro and hexacyano complexes of Cr^{III}, Fe^{II}, and Co^{III}. The d−d transition energies of calculated spectra differed from experimental spectra by amounts very similar to those observed for the hexaalkynyl complexes: $[CrCl_6]^{3-}$, +0.50; $[Cr(CN)_6]^{3-}$, +0.16; $[Fe(CN)_6]$,$^{4-}$ −0.84; and $[Co(CN)_6]^{3-}$, −0.38 eV.
(46) Comparison of UV−vis spectra for **2** in acetonitrile and benzene showed that the charge-transfer bands displayed little solvent dependence, unlike the spectra of complexes **1** and **3**.
(47) Beck, W.; Feldt, K. Z. *Anorg. Allg. Chem.* **1965**, *341*, 113.
(48) (a) Konig, E.; Schlafer, H. L. *Z. Physik Chem. NF*, **1962**, *34*, 355. (b) Gray, H. B.; Beach, N. A. *J. Am. Chem. Soc.*, **1963**, *85*, 2922.
(49) Verkade, J. G.; Piper, T. S. *Inorg. Chem.* **1963**, *2*, 944.

chromium(III), iron(II), and cobalt(III). We anticipate that this preparative method will be generalizable to the formation of such complexes for many other transition metal ions. The strong covalency and π-donating character established for the trimethylsilylacetylide ligand are promising signs for observing strong magnetic exchange coupling and rapid electron transfer through linear carbon bridges. Accordingly, it is hoped that the new complexes $[Cr(CCSiMe_3)_6]^{3-}$, $[Fe(CCSiMe_3)_6]$,$^{4-}$ and $[Co(CCSiMe_3)_6]^{3-}$ will be of utility in the synthesis of acetylenediide- and 1,3-butadiynediide-bridged clusters and solids. Investigations toward employing these and related species (e.g., $[(Me_3tacn)Cr(CCH)_3]$[30] and $[(cyclam)Cr(CCH)_2]^+$) for such purposes are currently underway.

Acknowledgment. This research was funded by NSF Grant No. CHE-0072691 and DOE Grant No. DE-FG03-01ER15257. We thank Prof. J. K. McCusker, Dr. J. E. Monat, and Dr. K. Durkin for helpful discussions.

Supporting Information Available: Additional views of the structures of **3**, **4**, and **5**; fits to the UV−visible absorption spectrum of **1**; and X-ray crystallographic files (CIF). This material is available free of charge via the Internet at http://pubs.acs.org.

IC051551Z